Electronic Supplementary Material (ESI) for Physical Chemistry Chemical Physics.

Supplementary Information

Polarized coherent emission outside high-symmetry points of dye-coupled plasmonic lattices

Diego Piccotti,[a] Mirko Trevisani,[a] Giuseppe Pirruccio,[b] Boris Kalinic,[a] Tiziana Cesca,*[a] and Giovanni Mattei[a]

[a] University of Padova, Department of Physics and Astronomy, NanoStructures Group, via Marzolo 8, I-35131 Padova, Italy.

E-mail: tiziana.cesca@unipd.it

[b] Instituto de Física, Universidad Nacional Autónoma de México, Apartado Postal 20-364, Mexico D.F. 01000, México

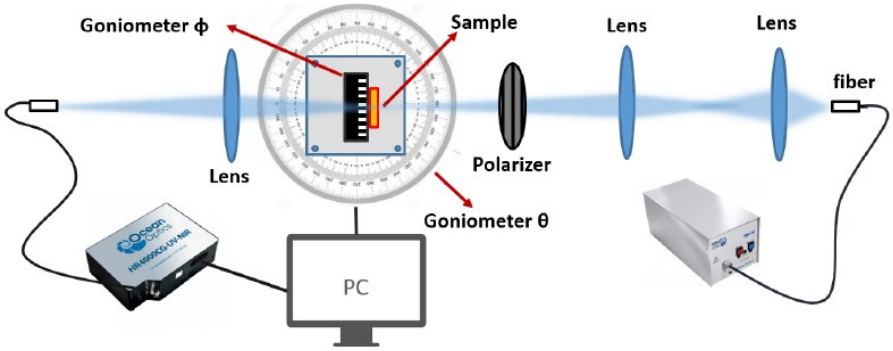

Figure S1 Set-up for angle-resolved extinction measurements.

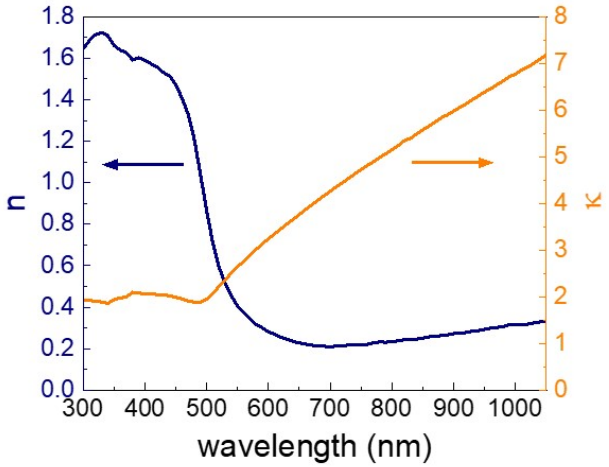

Figure S2 Experimental complex refractive index (n, κ) of Au thin film.

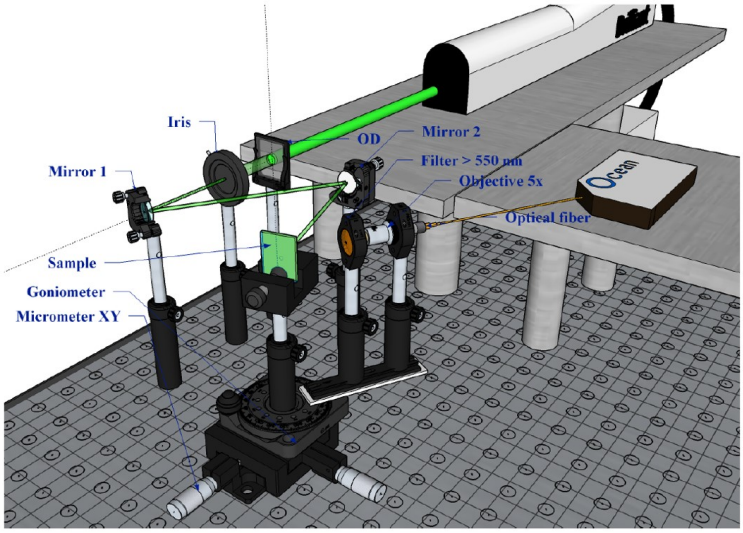

Figure S3 Set-up for angle-resolved photoluminescence measurements.

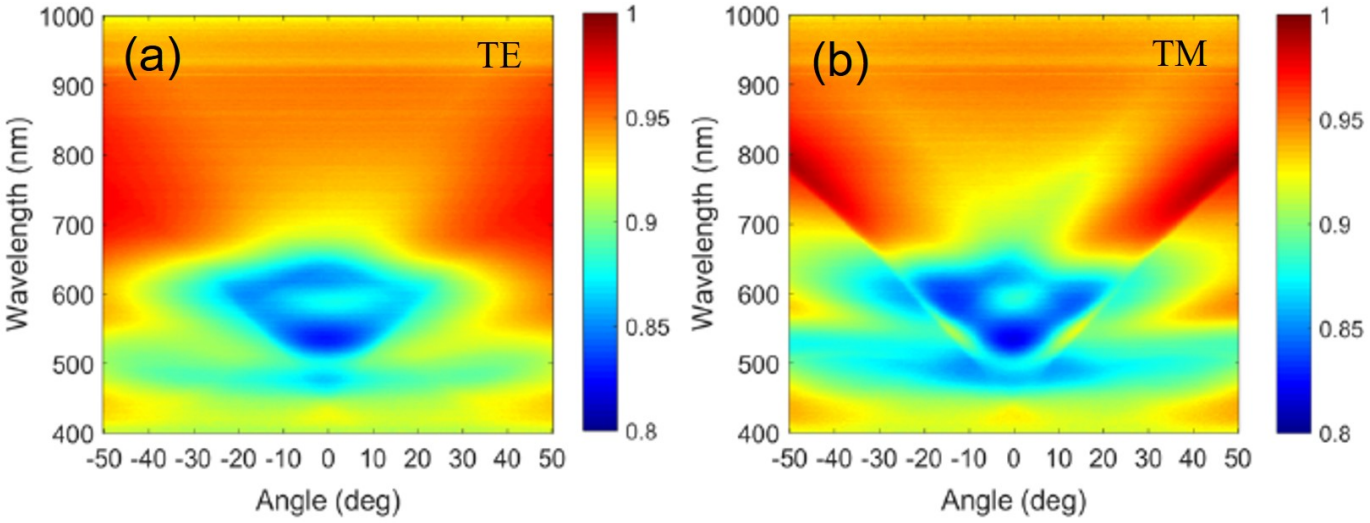

Figure S4 Experimental extinction (E=1-T) maps of the Au-HNDA in (a) TE and (b) TM polarization along the Γ-M direction, in air (n=1).

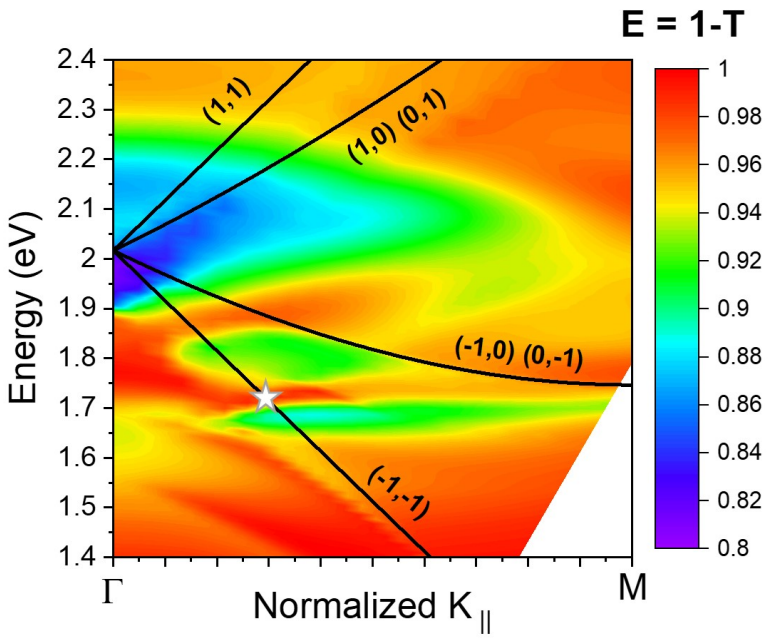

Figure S5 FEM simulated extinction (E=1-T) map of the Au-HNDA in ethanol taken in TM polarization along the Γ-M direction.

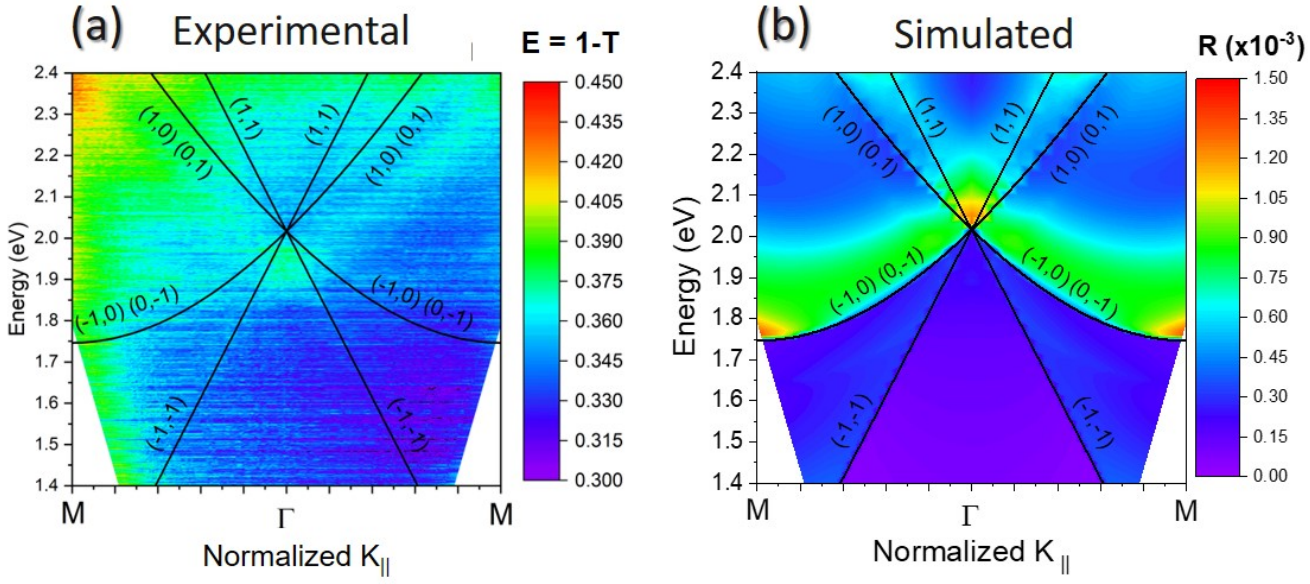

Figure S6 (a) Experimental extinction (E=1-T) map and (b) FEM simulated reflectance (R) map of the SiO_2-HNDA in ethanol, for TM polarization along the Γ-M direction. The black lines are the Rayleigh anomalies (see main text), labeled with the corresponding Miller indexes.

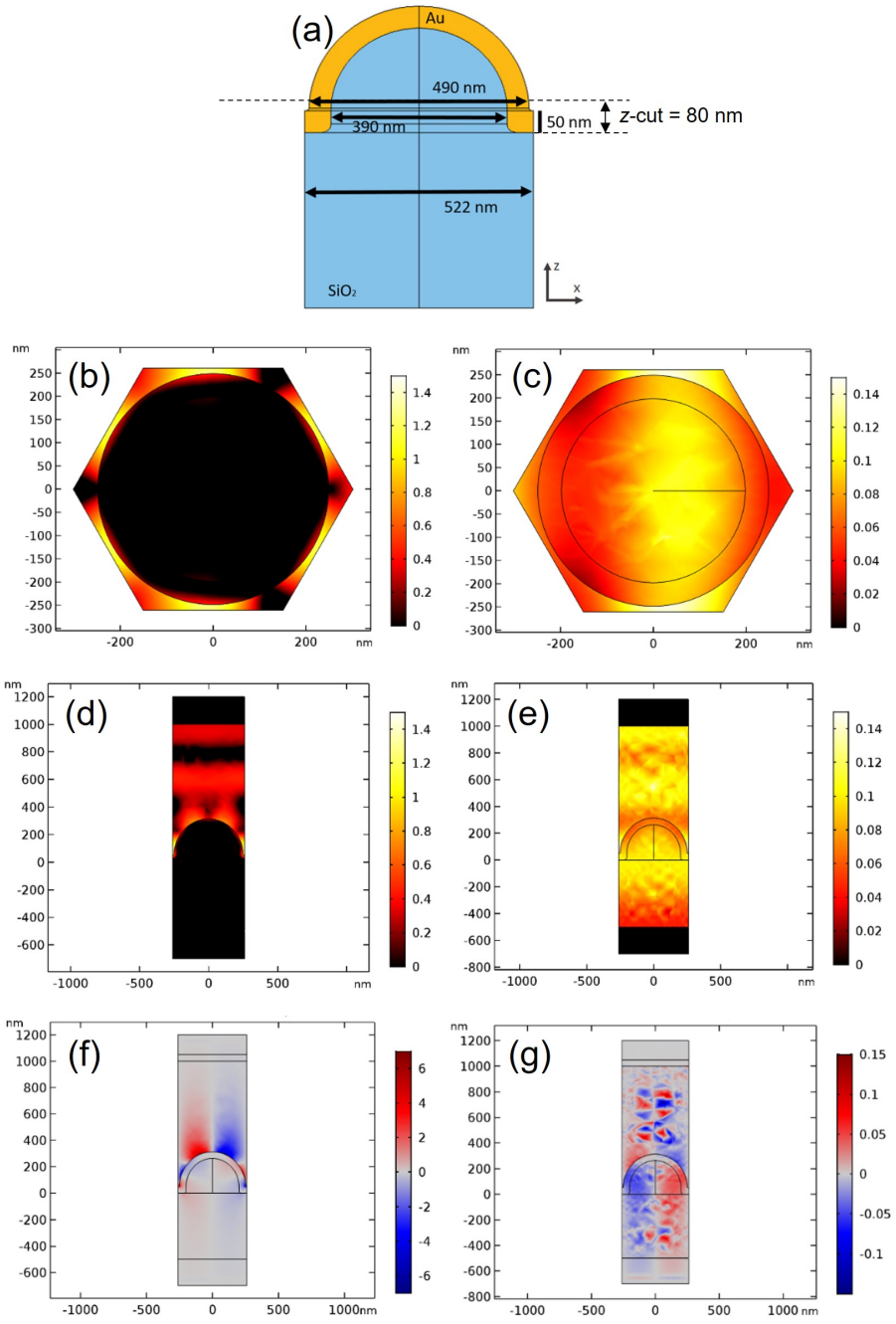

Figure S7 FEM simulations. (a) Main geometrical parameters of the FEM model of a gold nanodome; the sketch shows the $\hat{x}\hat{z}$ plane at $y = 0$. The same model was used for the silica nanodome. (b,c) Top-view ($\hat{x}\hat{y}$, $z = 80$ nm) and (d,e) side-view ($\hat{y}\hat{z}$, $x = 0$) of the maps of near-field enhancement factor in logarithmic scale, $\log(|\mathbf{E}|/E_0)$, for (b,d) the Au-HNDA and (c,e) the SiO_2-HNDA. The incident field is TE-polarized ($\mathbf{E}_0 // \hat{y}$). (f,g) Side-view ($\hat{y}\hat{z}$, $x = 0$) in linear scale of the maps of the $\hat{z}$ component (perpendicular to the array plane) of the electric field E_z, normalized to the incident field E_0, of (f) Au-HNDA and (g) SiO_2-HNDA. All the maps are simulated at the lasing emission condition ($\lambda = 723$ nm, emission angle 17° along the Γ-M direction).

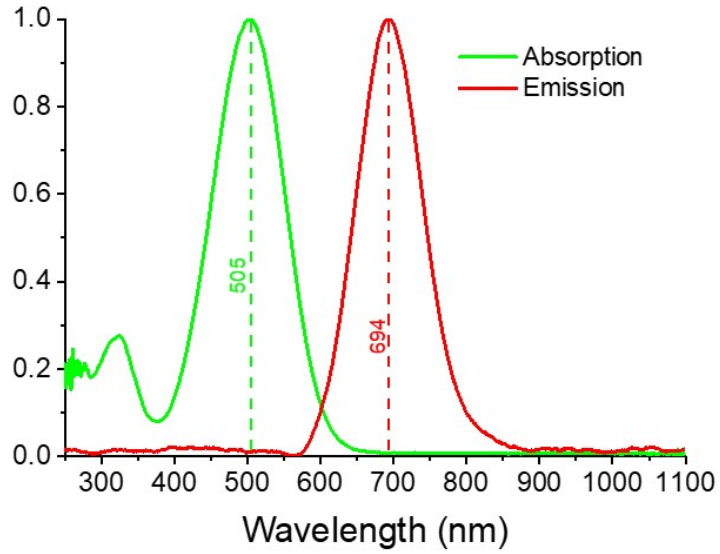

Figure S8 Normalized absorption and emission spectra of Pyridine 2 in ethanol.

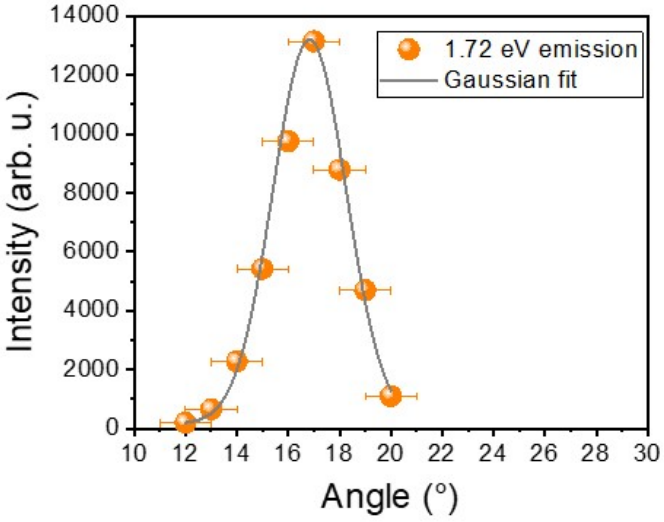

Figure S9 Angular scan along the Γ-M direction, of the 1.72 eV emission peak of sample Au-HNDA+Py2; the sample is excited at an angle of 50° with respect to the surface's normal, with a pump fluence of 1.4 mJ/cm^2. The gray curve is the Gaussian fit of the angular data.

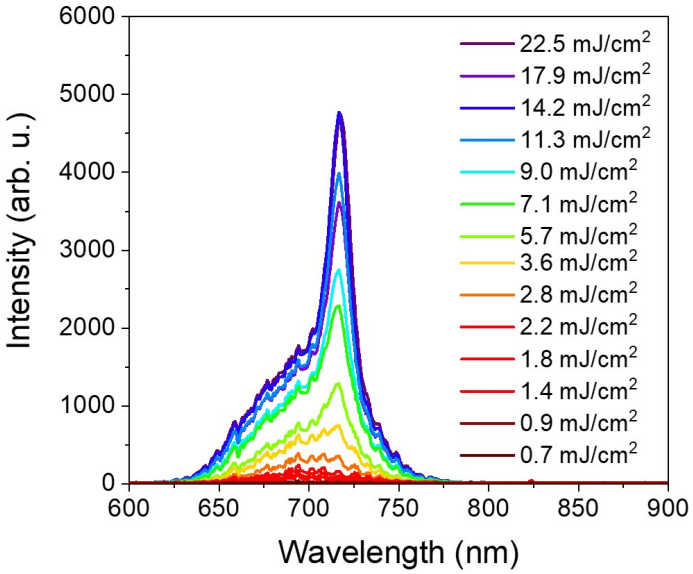

Figure S10 PL measurements as a function of the pump fluence of the sample SiO_2-HNDA+Py2; the sample is excited at an angle of 50° with respect to the surface's normal and the emission is collected at 17°.

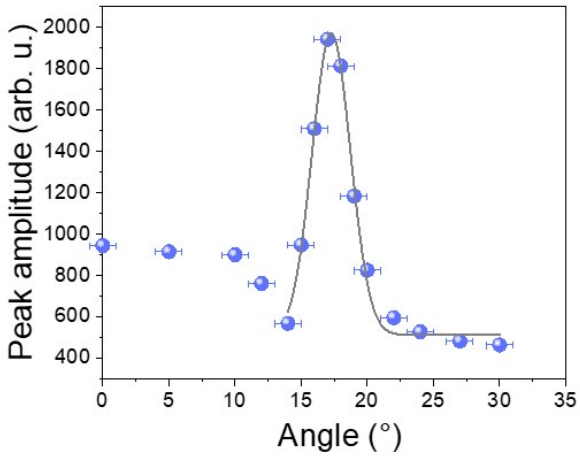

Figure S11 Angular scan along the Γ-M direction of the emission peak of sample SiO_2-HNDA+Py2; the sample was excited at an angle of 50° with respect to the surface's normal, with a pump fluence of 15.4 mJ/cm^2. The gray curve is the Gaussian fit of the angular data.

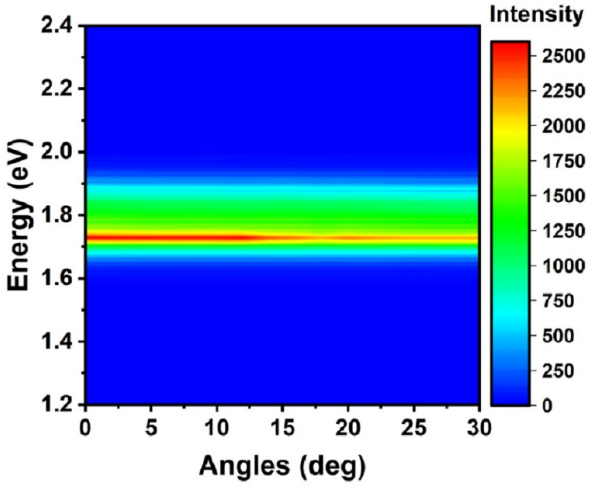

Figure S12 Angular emission map of Py2 dissolved in ethanol taken at an incidence angle of 50°, with a pump fluence of 15.4 mJ/cm^2.

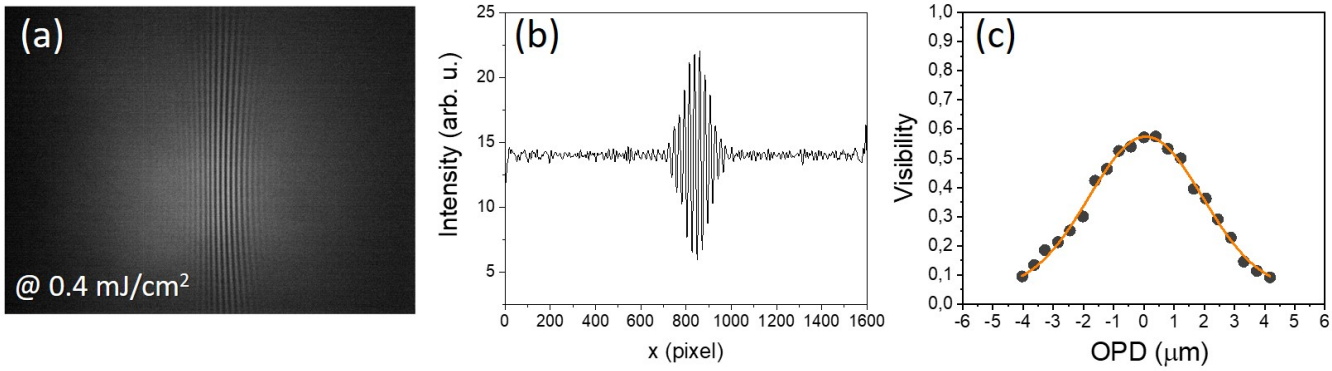

Figure S13 (a) Interference pattern recorded from the Au-HNDA+Py2 sample with an excitation fluence of 0.4 mJ/cm^2 (below threshold). (b) Intensity profile of the interference pattern in (a). (d) Fringe visibility (dots) as a function of the optical path distance (OPD); the orange curve is the Gaussian fit of the visibility data.